Active Matter in two dimensions

Leticia F. Cugliandolo

Sorbonne Université

Institut Universitaire de France

leticia@lpthe.jussieu.fr
www.lpthe.jussieu.fr/~leticia

Work in collaboration with

C. Caporusso, **G. Gonnella**, **P. Digregorio & I. Petrelli** (Bari, Italia)

A. Suma (Trieste, Italia, Philadelphia, USA & Bari, Italia)

D. Levis & I. Pagonabarraga (Barcelona, España & Lausanne, Suisse)

Buenos Aires 2023

Active matter

Definition

Active matter is composed of large numbers of active "agents", which consume energy and thus move or exert mechanical forces.

Due to the energy consumption, these systems are intrinsically out of thermal equilibrium.

Homogeneous energy injection (not from the borders, *cfr.* shear).

Coupling to the environment (bath) lets allows for dissipation

Active matter

Realisations & modelling

- Wide range of scales: macroscopic to microscopic

  Natural examples are birds, fish, cells, bacteria.

  Artificial realisations are Janus particles, asymmetric grains, toys, etc.

- Embedding spaces in $3d$, $\boxed{2d}$ and $1d$.

- Modelling: very detailed to coarse-grained or schematic:

  — microscopic or *ab initio* with focus on active mechanism,

  — *mesoscopic*, just forces that do not derive from a potential,

  — *Cellular automata* like in the Vicsek model.

Active matter

Natural & artificial systems

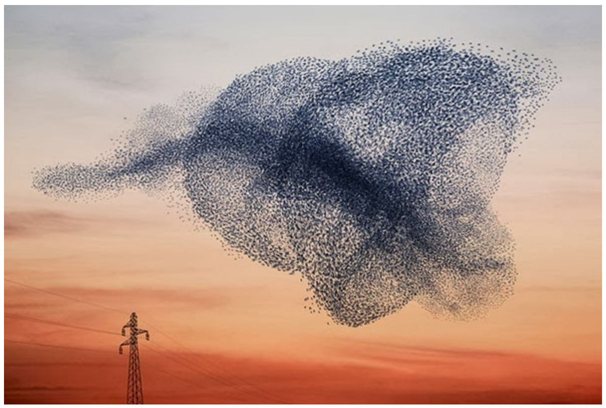

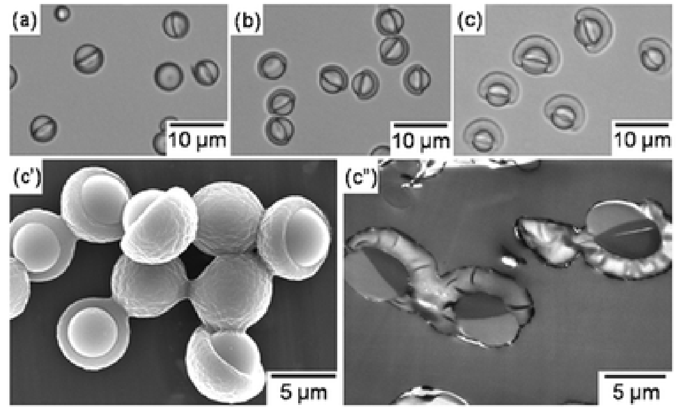

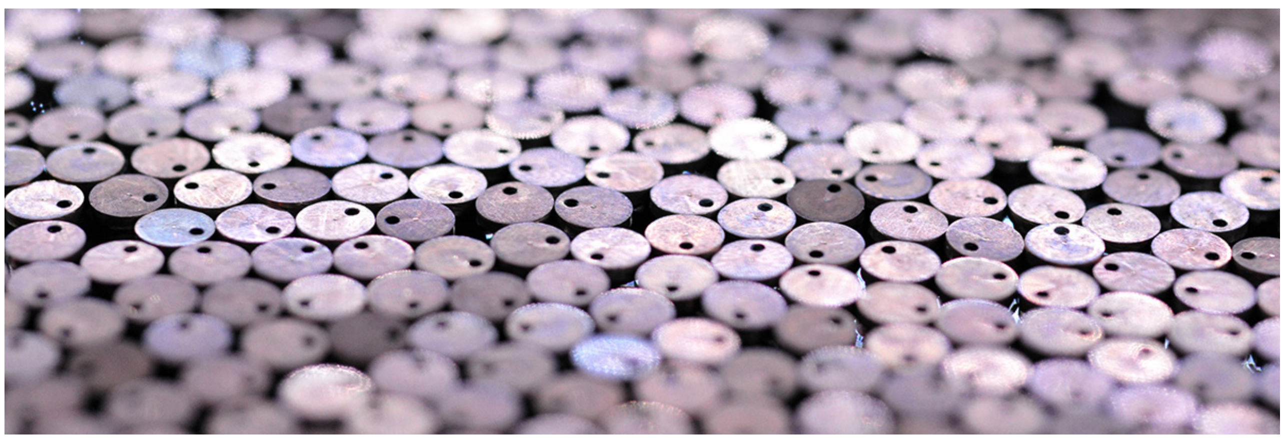

Experiments & observations **Bartolo et al.** Lyon, **Bocquet et al.** Paris, **Cavagna et al.** Roma, **di Leonardo et al.** Roma, **Dauchot et al.** Paris, just to mention some Europeans

Active matter

Realisations & modelling

- Wide range of scales: macroscopic to microscopic

  Natural examples are birds, fish, cells, bacteria.

  Artificial realisations are Janus particles, asymmetric grains, toys, etc.

- Embedding spaces in $3d$, $\boxed{2d}$ and $1d$.

- Modelling: very detailed to coarse-grained or schematic:

  — microscopic or *ab initio* with focus on active mechanism,

  — *mesoscopic*, just forces that do not derive from a potential,

  — *Cellular automata* like in the Vicsek model.

Active Brownian Disks in $2d$

(Overdamped) Langevin equations (the standard model)

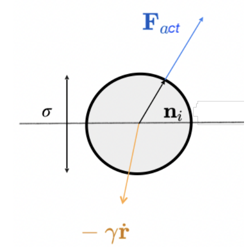

Active force $\mathbf{F}_{\rm act}$ along $\mathbf{n}_i = (\cos\theta_i, \sin\theta_i)$

$$m\ddot{\mathbf{r}}_i + \gamma\dot{\mathbf{r}}_i = F_{\rm act}\mathbf{n}_i - \nabla_i \sum_{j(\neq i)} U_{\rm Mie}(r_{ij}) + \boldsymbol{\xi}_i \ , \qquad \dot{\theta}_i = \eta_i \ ,$$

$\mathbf{r}_i$ position of ith particle & $r_{ij} = |\mathbf{r}_i - \mathbf{r}_j|$ inter-part distance,

$U_{\rm Mie}$ short-range **repulsive** Mie potential, over-damped limit $m \ll \gamma$

$\boldsymbol{\xi}$ and η zero-mean Gaussian noises with

$\langle \xi_i^a(t)\, \xi_j^b(t')\rangle = 2\gamma k_B T \delta_{ij}^{ab}\delta(t-t')$ and $\langle \eta_i(t)\, \eta_j(t')\rangle = 2D_\theta\delta_{ij}\delta(t-t')$

The units of length, time and energy are given by σ, $\tau_p = D_\theta^{-1}$ and ε

$D_\theta = 3k_BT/(\gamma\sigma^2)$ controls persistence, $\gamma/m = 10$ and $k_BT = 0.05$

Péclet number Pe = $F_{\rm act}\sigma/(k_BT)$ and $\phi = \pi\sigma^2 N/(4S)$, measures activity

Active Brownian disks

The typical motion of particles in interaction

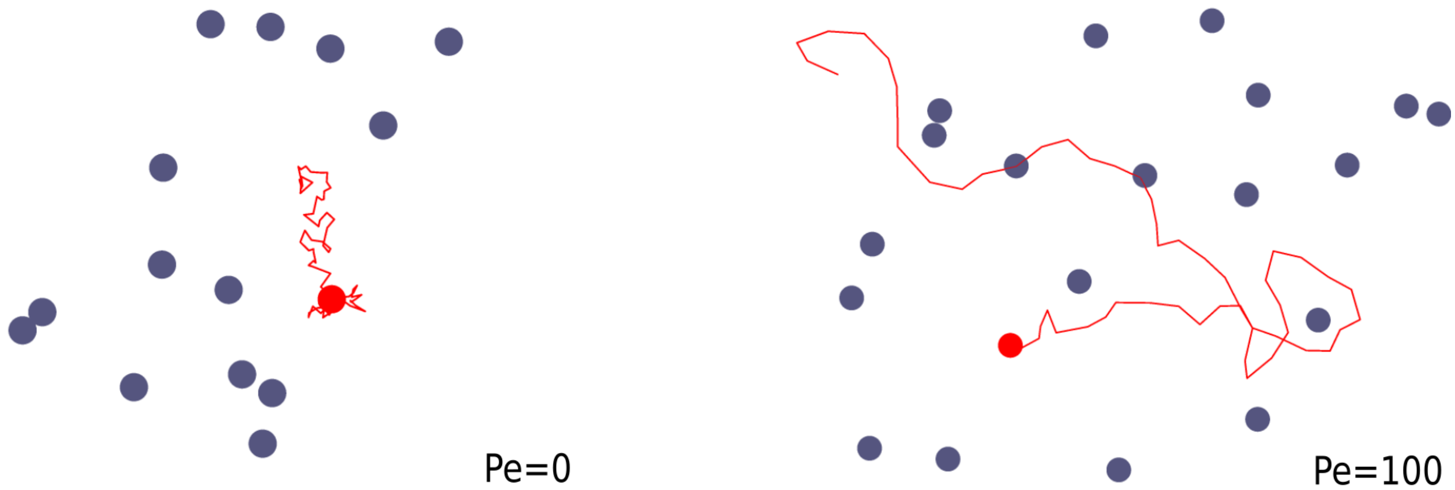

The active force induces a persistent random motion due to

$$\langle \mathbf{F}_{\rm act}(t) \cdot \mathbf{F}_{\rm act}(t') \rangle \propto F_{\rm act}^2 \, e^{-(t-t')/\tau_p}$$

with $\tau_p = D_\theta^{-1}$

Active Brownian disks

Questions

- Pe - ϕ Phase diagram
- Mechanisms for phase transitions.
- Topological defects.
- Dynamics across phase transitions.
- Motility Induced Phase Separation.

- Influence of particle shape, *e.g.* disks *vs.* dumbbells.

Active Brownian disks

Questions

- Pe - ϕ Phase diagram – start from solid and dilute
- Mechanisms for phase transitions.
- Topological defects.
- Dynamics across phase transitions.
- Motility Induced Phase Separation.

- Influence of particle shape, *e.g.* disks *vs.* dumbbells.

Freezing/Melting

Two step route in passive Pe = 0 $2d$ systems

$T = 0$ Position & orientation order lost

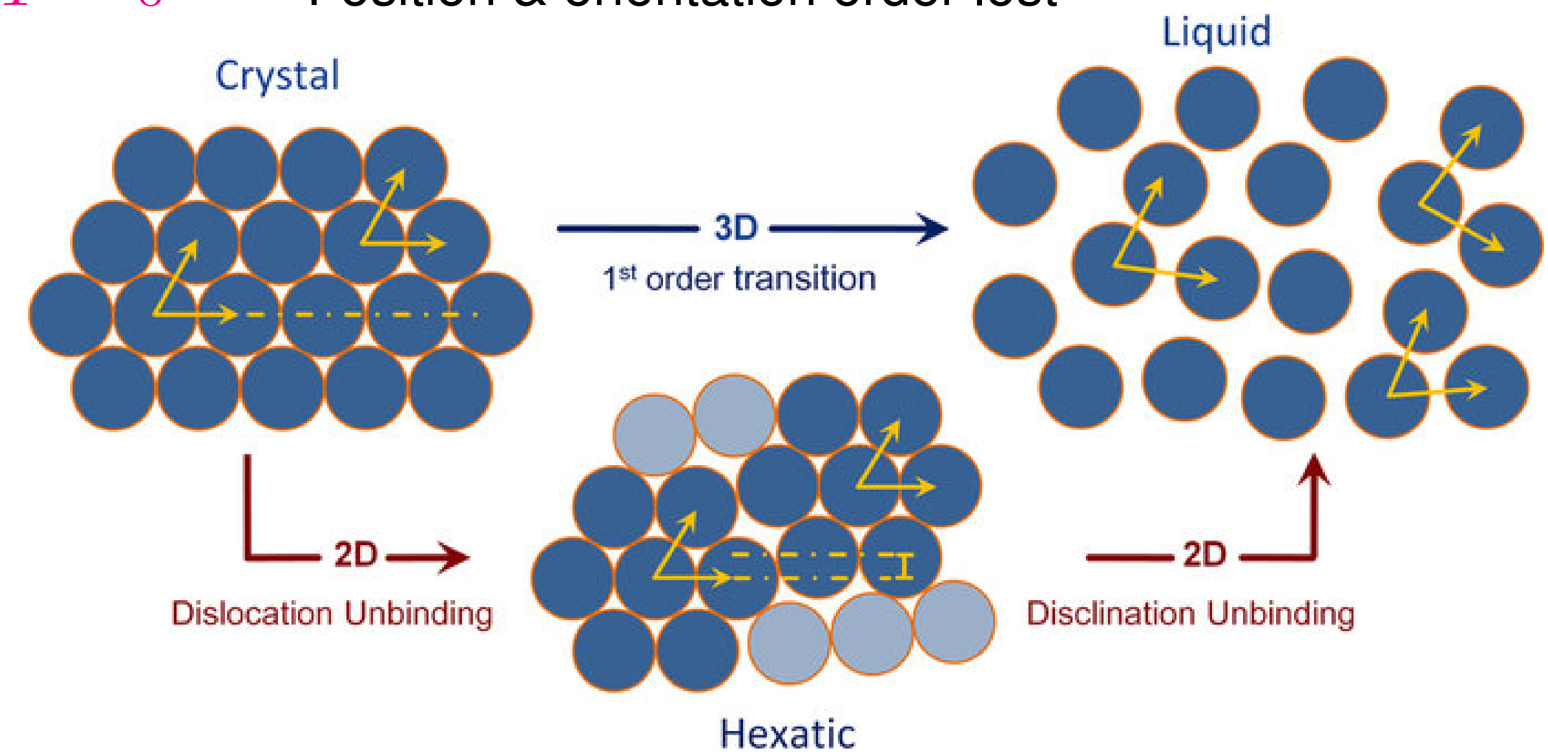

Orientation order preserved also lost

Image from **Pal, Kamal & Raghunathan, Sc. Rep. 6, 32313 (2016)**

Freezing/Melting

Hexatic (orientational) order $\psi_{6j} = nn_j^{-1} \sum_{k=1}^{nn_j} e^{i6\theta_{jk}}$

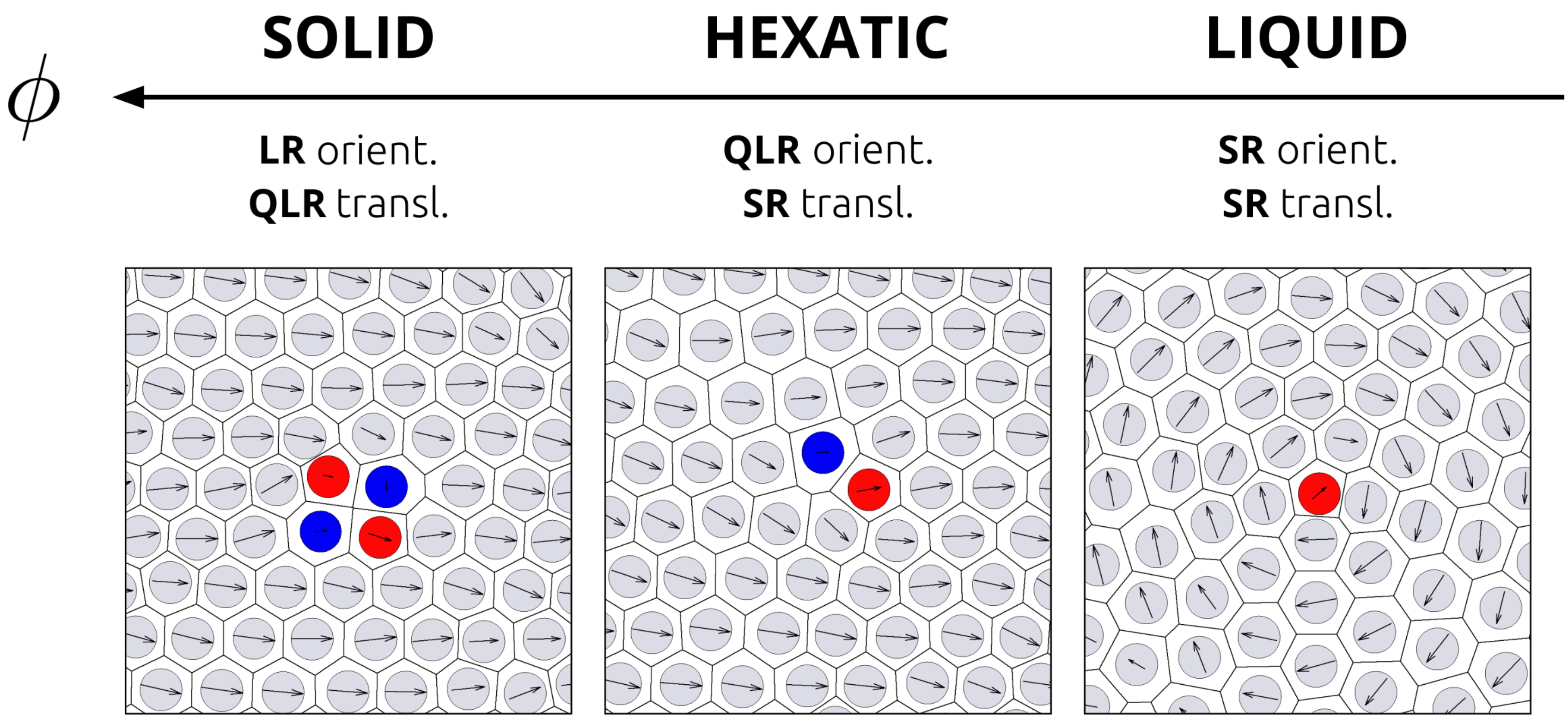

arrows oriented (LR) less oriented (QLR) order lost (SRL)

● five neighbours ● seven neighbours

Voronoi tessellation

Phase Diagram

Solid, hexatic, liquid, co-existence and MIPS

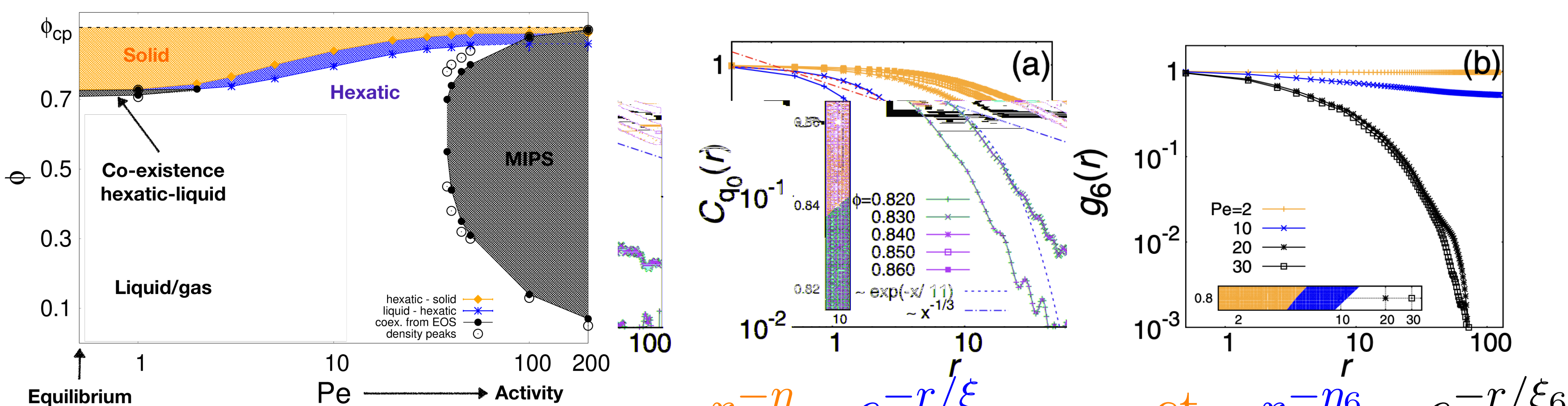

$r^{-\eta}$ $e^{-r/\xi}$ ct $r^{-\eta_6}$ e^{-r/ξ_6}

First order **liquid** - **hexatic** transition & co-existence at low Pe from

Pressure $P(\phi, \text{Pe})$ (EoS)

Distributions of ϕ_i and $|\psi_{6i}|$

Phases characterized by

Translational correlations $C_{q_0}(r)$ & orientational order correlations $g_6(r)$

Digregorio, Levis, Suma, LFC, Gonnella & Pagonabarraga, PRL 121, 098003 (2018)

Freezing/Melting

Mechanisms in $2d$ passive systems : defects

ϕ ←

SOLID	HEXATIC	LIQUID
LR orient.	**QLR** orient.	**SR** orient.
QLR transl.	**SR** transl.	**SR** transl.

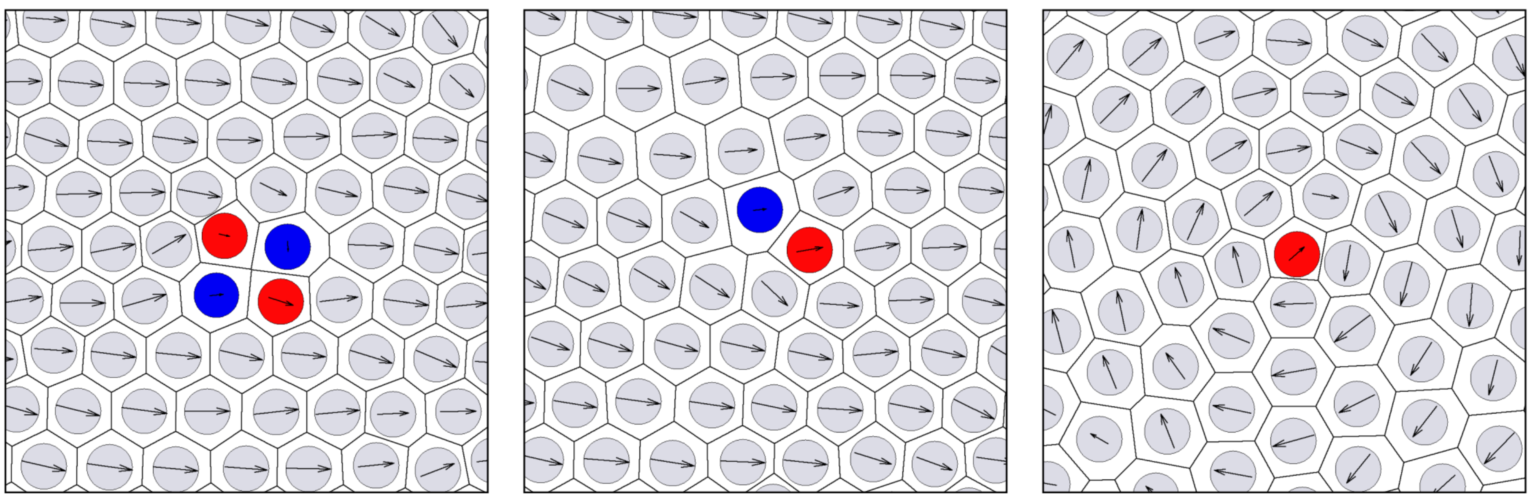

Confined dislocations   dislocations unbind   disclinations unbind

● five neighbours   ● seven neighbours

Voronoi tessellation

Active Brownian disks

Phase diagram with solid, hexatic, liquid, co-existence and MIPS

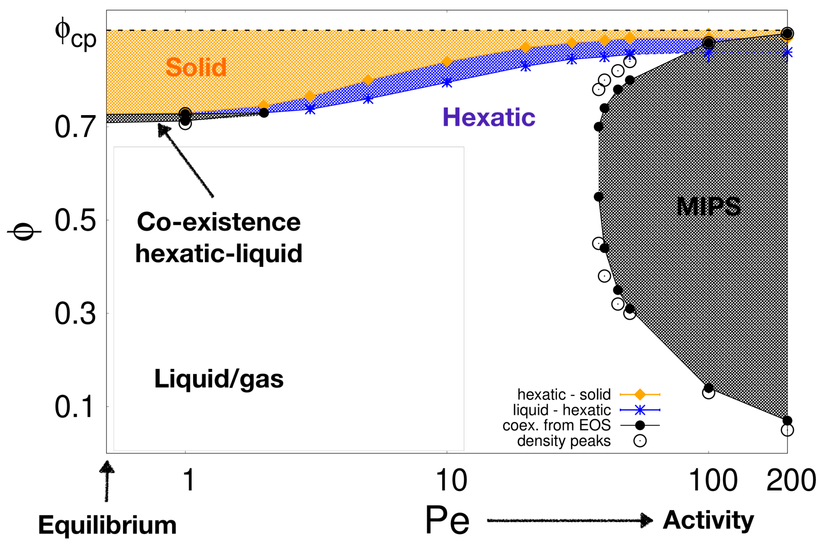

1st order **hexatic-liquid** close to Pe = 0

KT-HNY **solid-hexatic** dislocation unbinding

disclination unbinding in liquid

percolation of defect clusters in liquid

Pressure $P(\phi, \mathrm{Pe})$ (EOS), correlations $C_{q_0}(r)$, $g_6(r)$, and distributions of ϕ_i, $|\psi_{6i}|$

defect identification & counting

Digregorio, Levis, Suma, LFC, Gonnella & Pagonabarraga, PRL 121, 098003 (2018)

Digregorio, Levis, LFC, Gonnella & Pagonabarraga, Soft Matter 18, 566 (2022)

Topological defects

Summary of results

- **Solid** - **hexatic** à la BKT-HNY even quantitatively (ν value) and independently of the activity (Pe) *Universality*

- **Hexatic** - **liquid** very few disclinations and not even free.
  Breakdown of the BKT-HNY picture for all Pe (even zero)

- Close to, but in the liquid, **percolation** of *clusters of defects* with properties of uncorrelated critical percolation ($d_{\rm f}, \tau$)

- In **MIPS**, network of defects on top of the interfaces between hexatically ordered regions, interrupted by the *gas bubbles in cavitation*

Mechanisms

Unbinding of defects ?

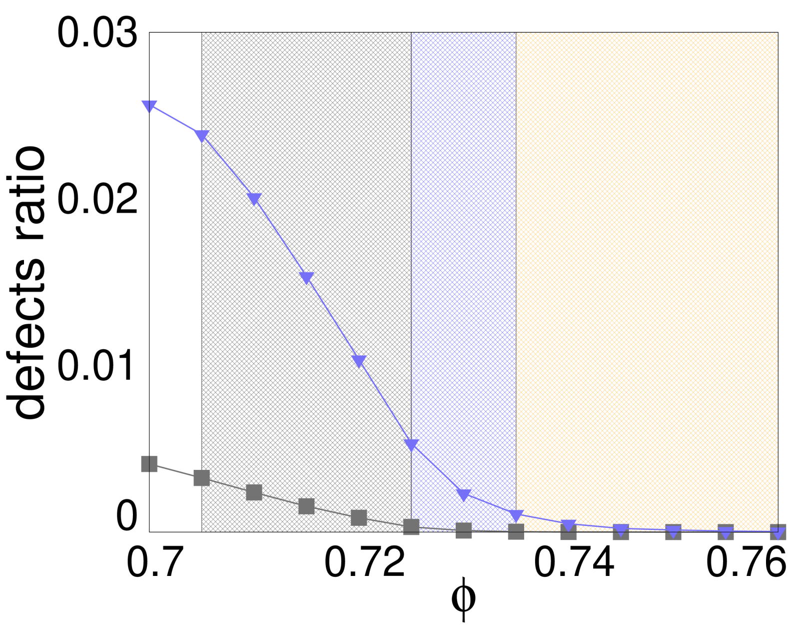

5 & 7 neighbors

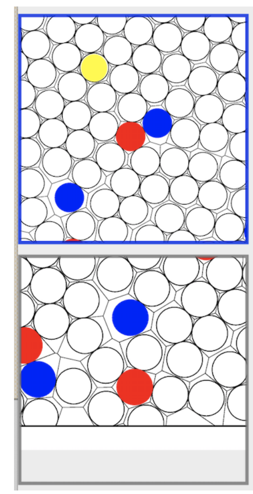

Dislocations ▼

Disclinations ■

Dislocations ▼ unbind at the **solid** - **hexatic** transition as in BKT-HNY theory

$$\rho_{dislocations} \sim a \ \exp\left[-b\left(\frac{\phi_c}{\phi_c-\phi}\right)^{\nu}\right] \qquad \nu \sim 0.37$$

Disclinations ■ unbind when the **liquid** appears in the co-existence region

Digregorio et al. Soft Matter 18, 566 (22) ; experiments Han, Ha, Alsayed & Yodh, PRE 77, 041406 (08)

Dislocations

At the solid-hexatic transition for all Pe $\nu = 0.37$ Universality

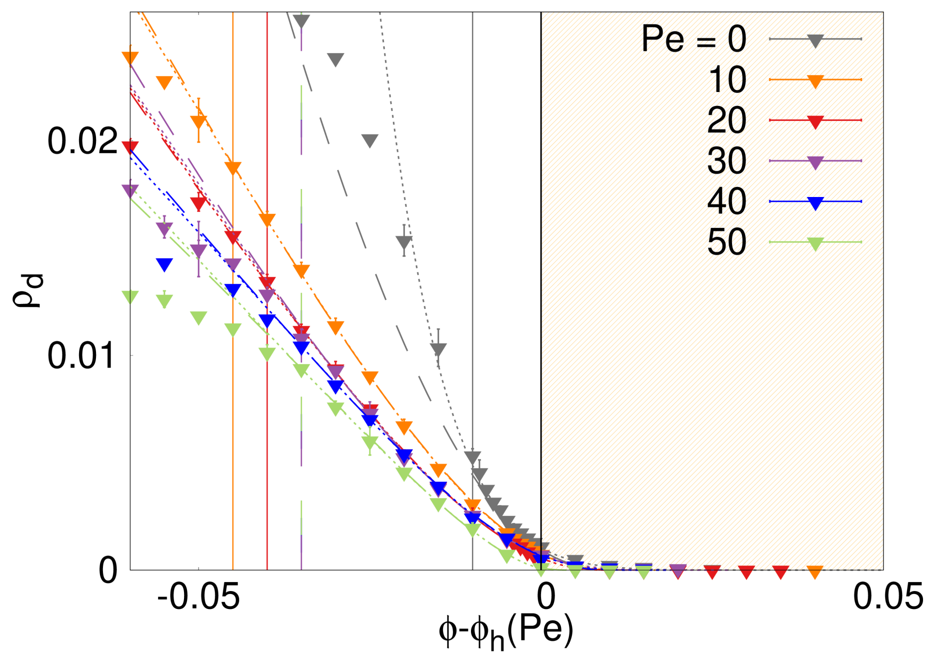

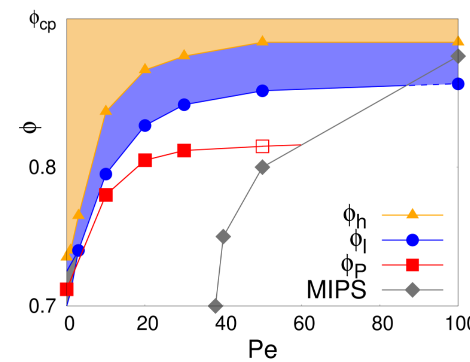

Four (ϕ_c, ν, a, b dotted) vs. three ($\phi_c, \nu = 0.37, a, b$ dashed) parameter fits on data in the hexatic & solid phases only. Criteria to support $\nu = 0.37$:

– χ^2 *cfr.* **Batrouni et al** for $2d$XY

– not crazy values for a, b but crazy values for ν if let to be fitted

– difference between ϕ_c and ϕ_h erased by coarse-graining

Disclinations

At the hexatic - liquid transition ϕ_l at all Pe

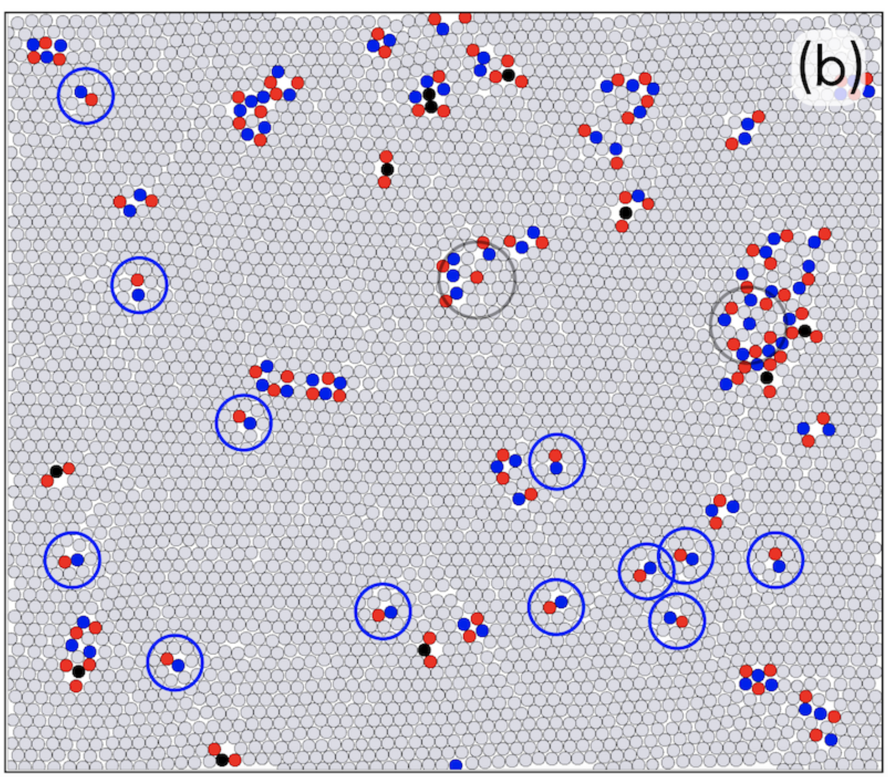

dislocations

disclinations

Very few disclinations, and always very close to other defects, so **not free**

Clusters

Close to the hexatic - liquid transition

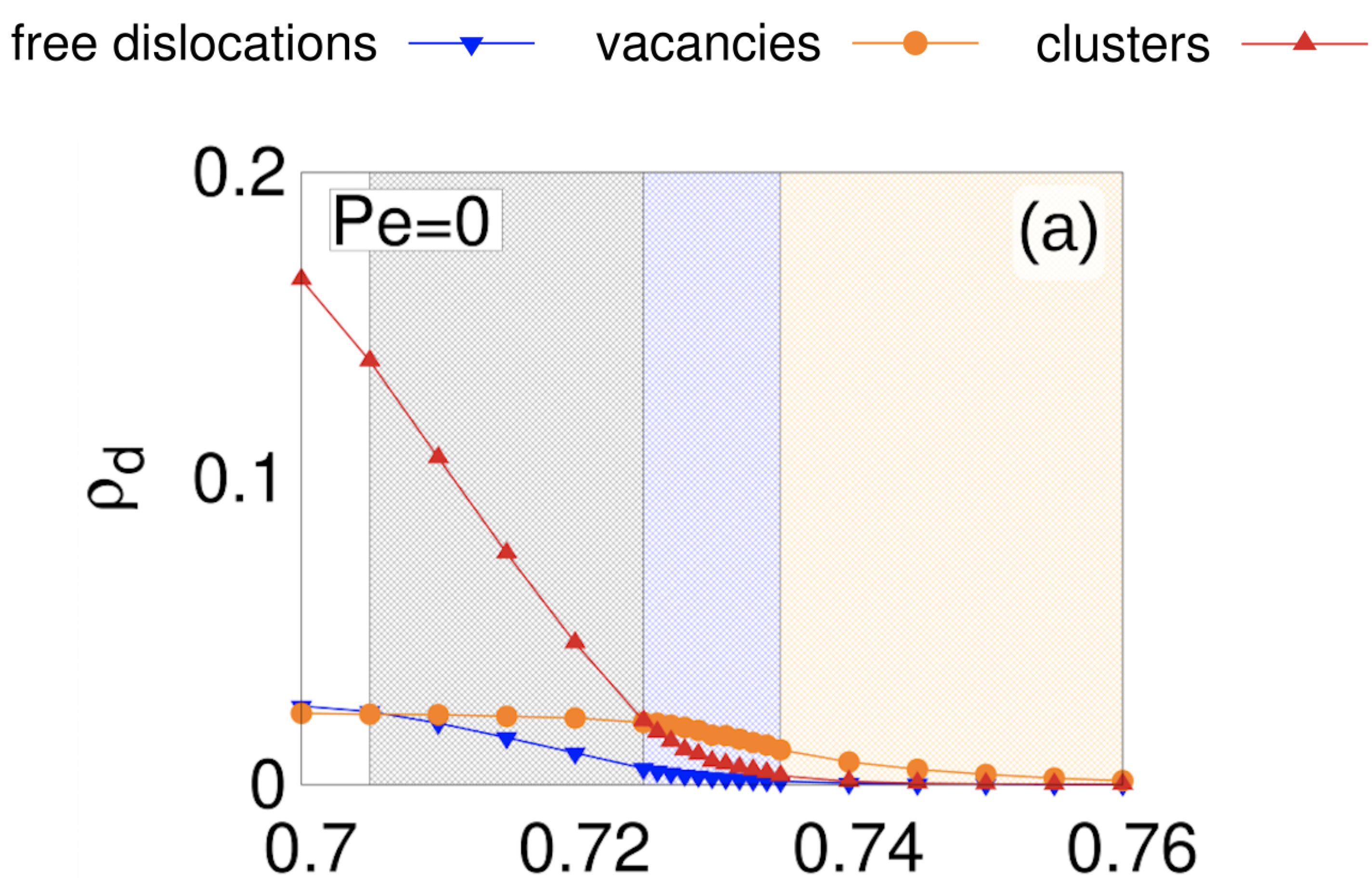

As soon as the liquid appears in co-existence, **defects in clusters dominate**

Clusters

Percolation of defect clusters : the critical curve

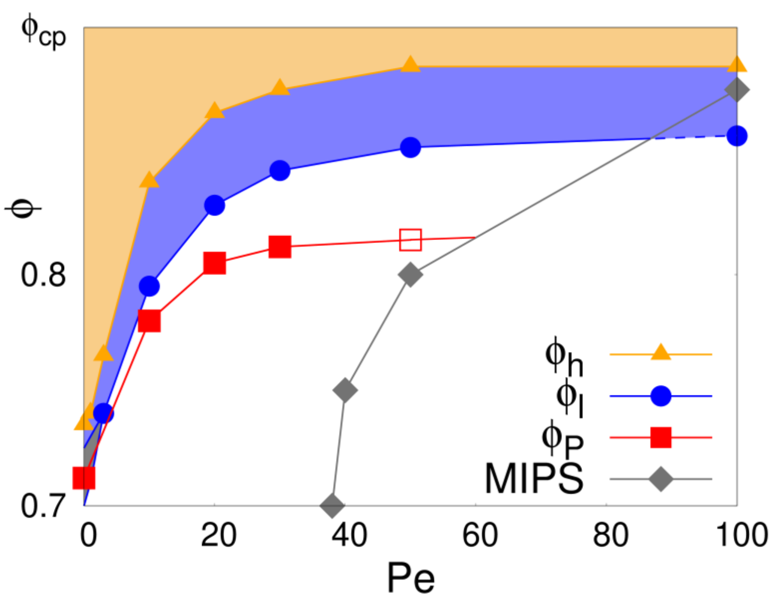

Critical percolation with

fractal properties $d_f \sim 1.9$ and

corresponding algebraic size distribution $\tau \sim 2.05$

With some coarse-graining the percolation curve moves upward towards the **hextic**-**liquid** critical one

Active Brownian disks

Questions

- Pe - ϕ Phase diagram.
- Mechanisms for phase transitions.
- Topological defects.
- Dynamics across phase transitions.
- Motility Induced Phase Separation.

- Influence of particle shape, *e.g.* disks *vs.* dumbbells.

Active Brownian disks

Phase diagram with solid, hexatic, liquid, co-existence and MIPS

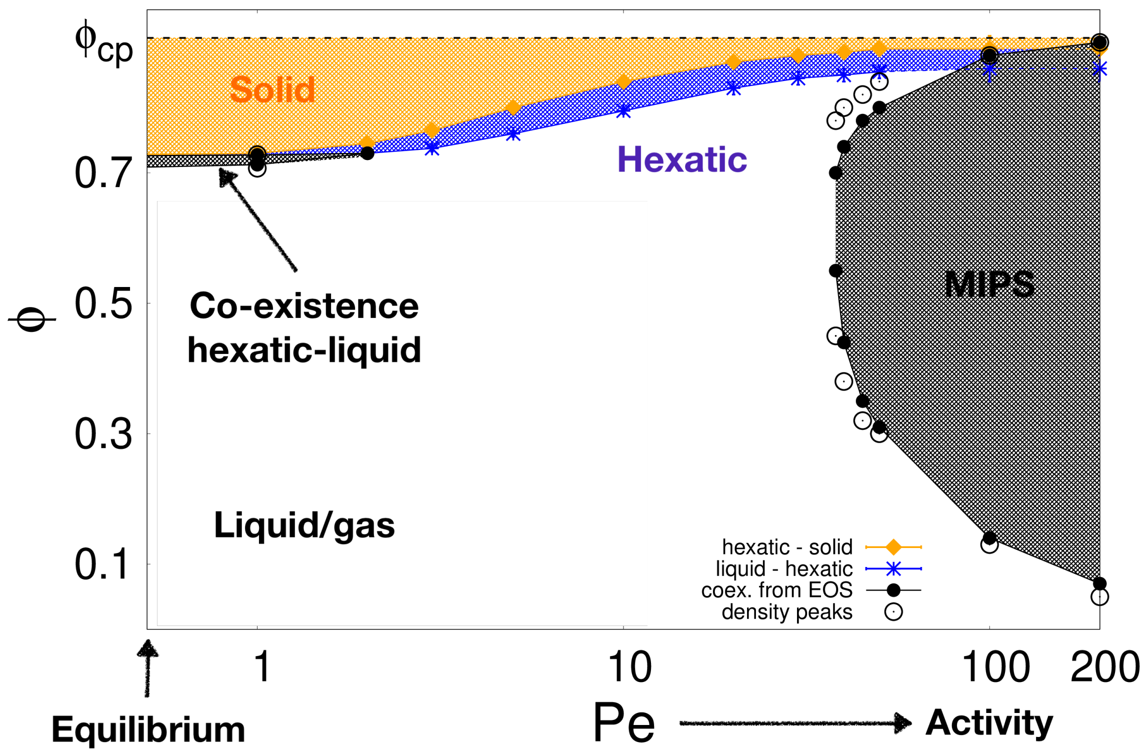

Motility induced

phase separation (MIPS)

gas & dense

Cates & Tailleur

Ann. Rev. CM 6, 219 (2015)

Farage, Krinninger & Brader

PRE 91, 042310 (2015)

Pressure $P(\phi, \text{Pe})$ (EOS), correlations $G_T(r)$, $G_6(r)$, and distributions of ϕ_i, $|\psi_{6i}|$

Digregorio, Levis, Suma, LFC, Gonnella & Pagonabarraga, PRL 121, 098003 (2018)

Motility Induced Phase Separation

The basic mechanism

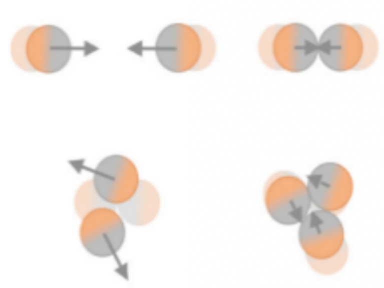

Particles collide heads-on

and cluster even in the

absence of attractive forces

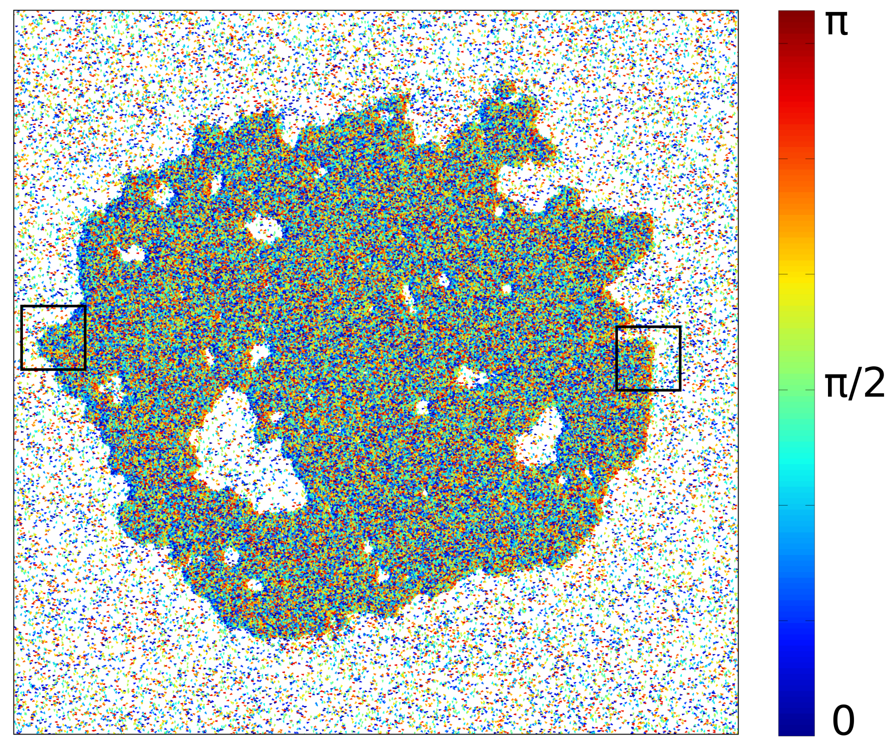

$\longrightarrow$ **blue 0** $\longleftarrow$ **red π**

The colours indicate the direction along which the particles are pushed by the active force $\boldsymbol{F}_{\rm act}$

MIPS

Particle orientation at the borders

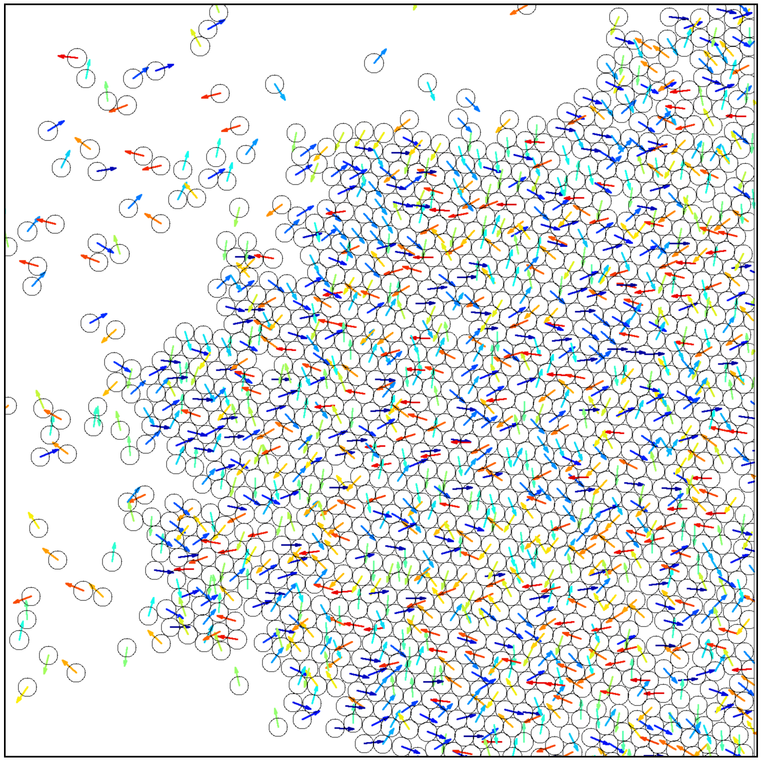

Zoom over **left border** $\rightarrow 0$

MIPS

Particle orientation at the borders

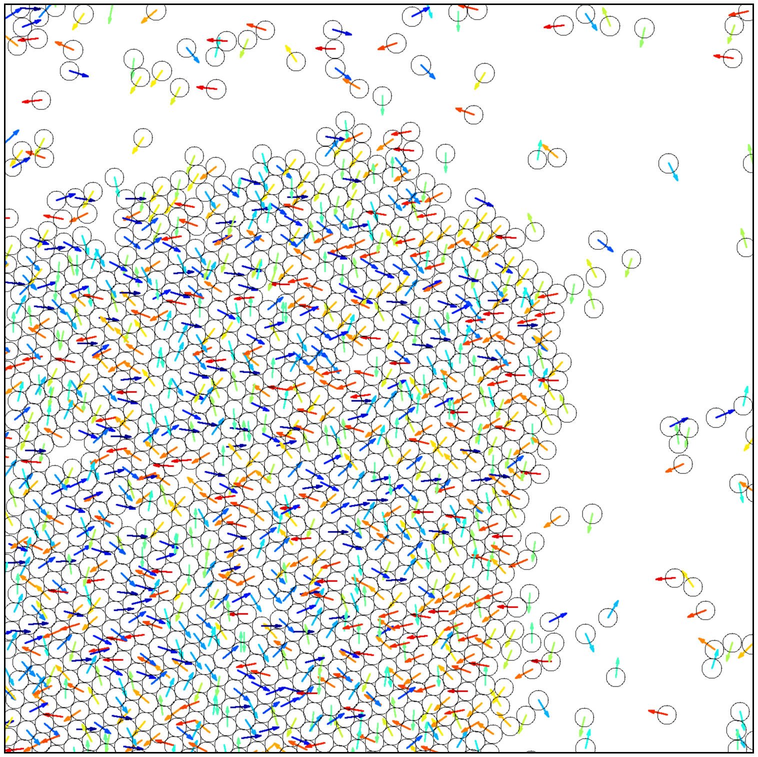

Zoom over **right border** $\leftarrow \pi$

MIPS

Local density distributions - dense & gas

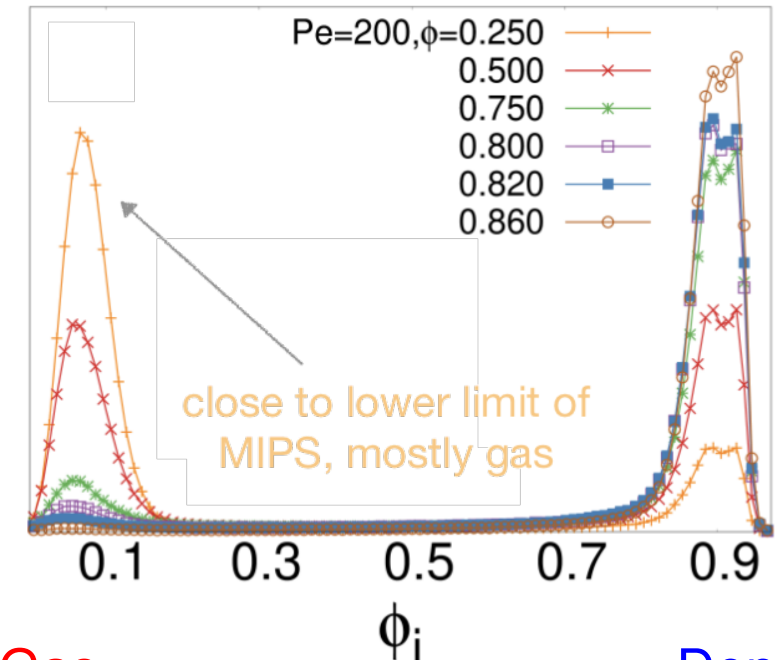

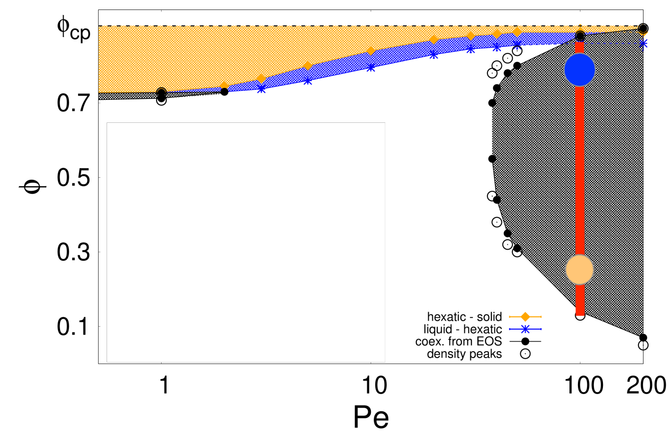

Gas Dense

The position of the peaks does not change while changing the global packing fraction ϕ but their relative height does. Transfer of mass from gas to dense component as ϕ increases

MIPS

Is it just a conventional phase separation ?

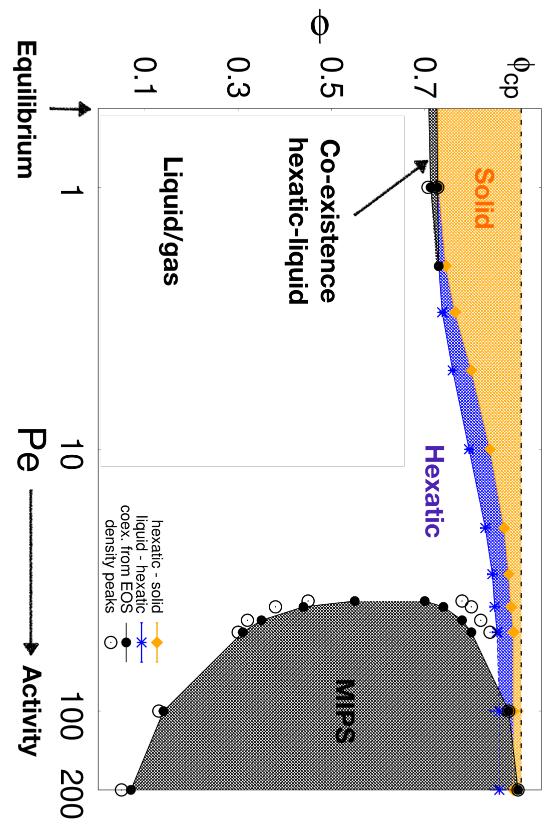

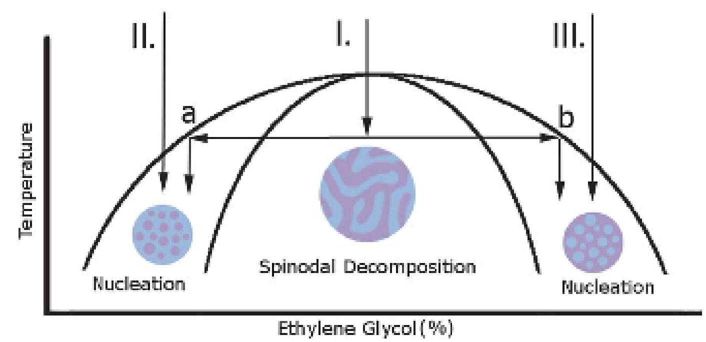

Similar to phase separation with percentage of system covered by dense and gas phases determined by a level rule ?

Cates & Tailleur 12

The dense phase

Hexatic patches, defects, bubbles

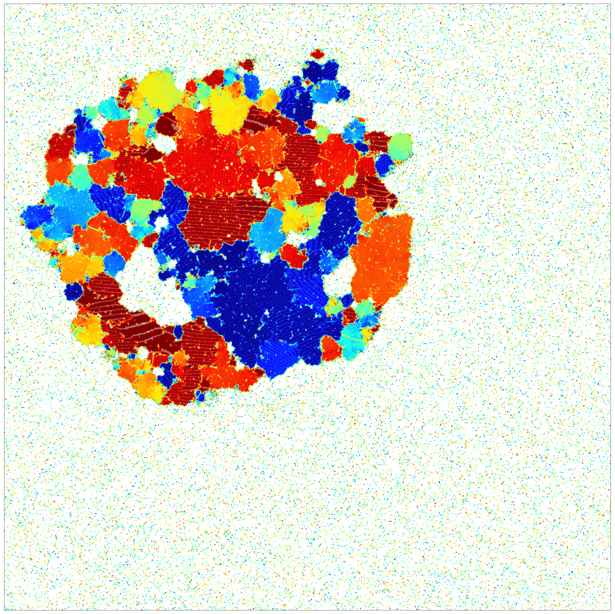

Dense/dilute separation[1]

For low packing fraction ϕ

a single round droplet

Growth[2,3] of a mosaic of

hexatic orders[3] with

gas bubbles[3,4,5] & defects[6]

[1] **Cates & Tailleur, Annu. Rev. Cond. Matt. Phys. 6, 219 (2015)**

[2] **Caporusso, Digregorio, LFC, Gonnella, Levis & Suma, in preparation**

[3] **Caporusso, Digregorio, Levis, LFC & Gonnella, PRL 125, 178004 (2020)**

[4] **Tjhung, Nardini & Cates, PRX 8, 031080 (2018)**

[5] **Shi, Fausti, Chaté, Nardini & Solon, PRL 125, 168001 (2020)**

[6] **Digregorio, Levis, LFC, Gonnella & Pagonabarraga, Soft Matter 18, 566 (2022)**

Structure

Dynamic structure factor ⇒ growing length of dense component

I peak:
system average
size

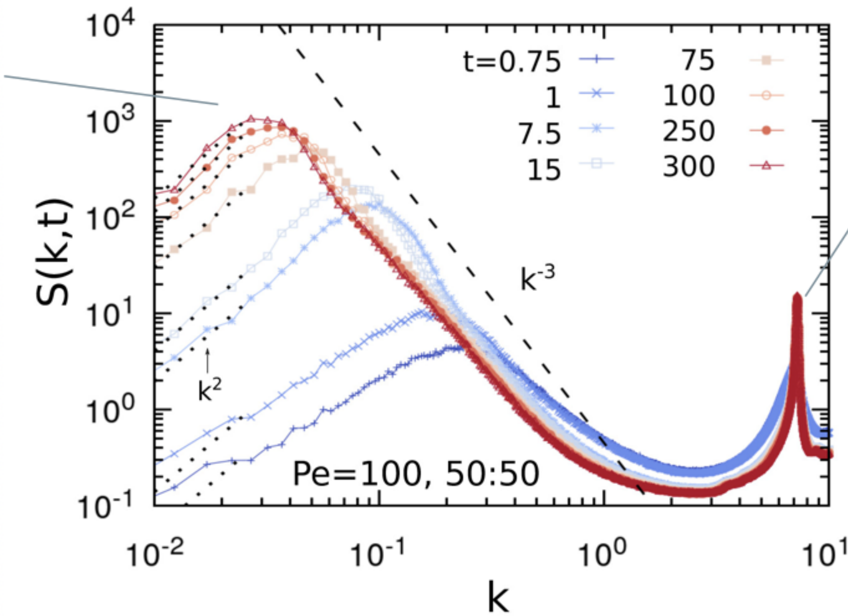

II peak:
particles' packing

$$S(\mathbf{k},t) = \sum_{i=1}^{N} e^{i\mathbf{k}(\mathbf{r_i}-\mathbf{r_j})}$$

related to Fourier transform of
the pair correlation function

$$k_{\mathrm{I}}(t) \propto R^{-1}(t)$$

No sign of fractality here. Porod's law $S(k) \sim k^{-(d+1)}$ for compact domains with sharp interfaces

The growth law

Growing length and regimes

Different Pe

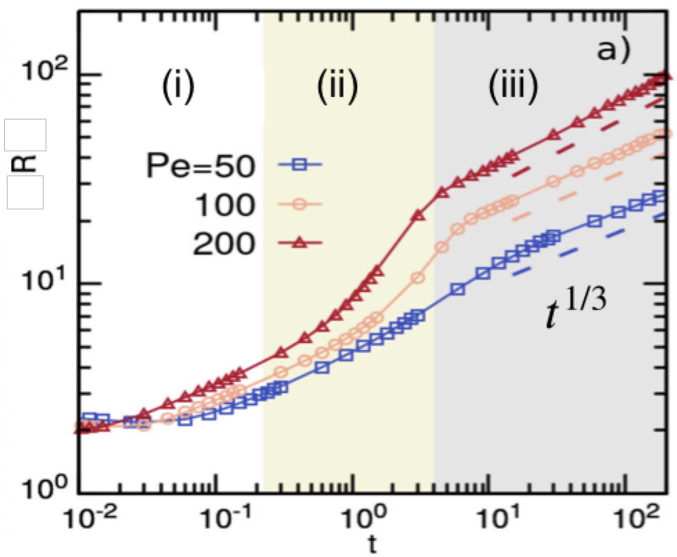

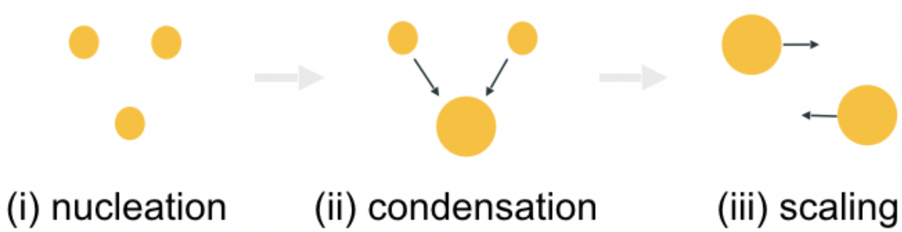

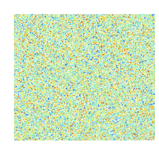

In scaling regime $t^{1/3}$ like in **Lifshitz-Slyozov-Wagner**, scalar phase separation.

More about it & asymptotic value later

Internal structure

The coloured patches

Local hexatic order parameter video

Orientational order

Local hexatic order parameter

$$\psi_{6j} = \frac{1}{nn_j} \sum_{k=1}^{nn_j} e^{i6\theta_{jk}}$$

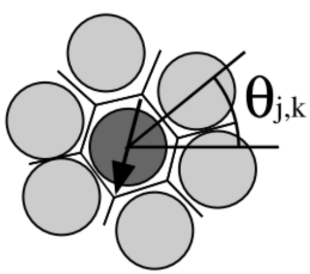

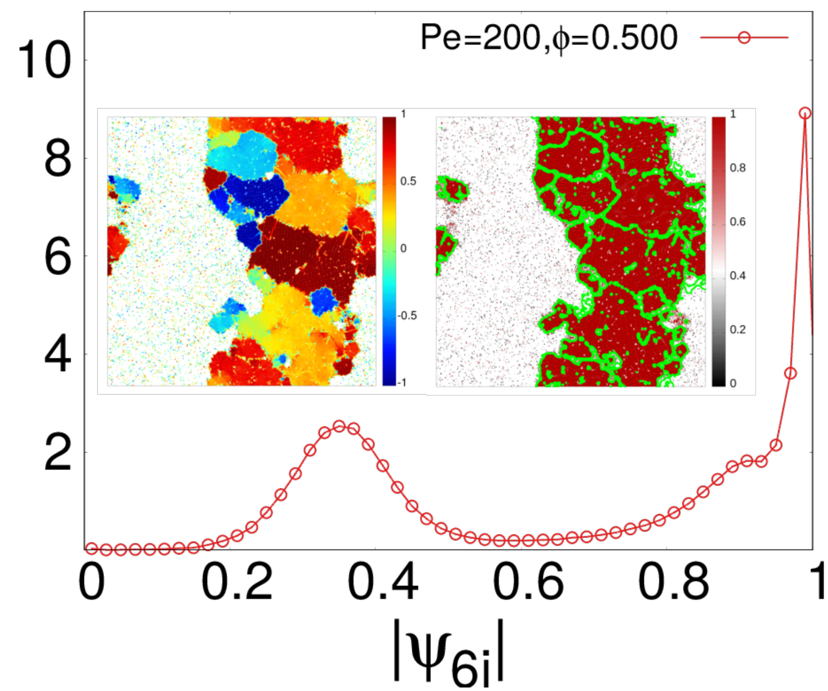

gas dense

Local hexatic order

Regimes

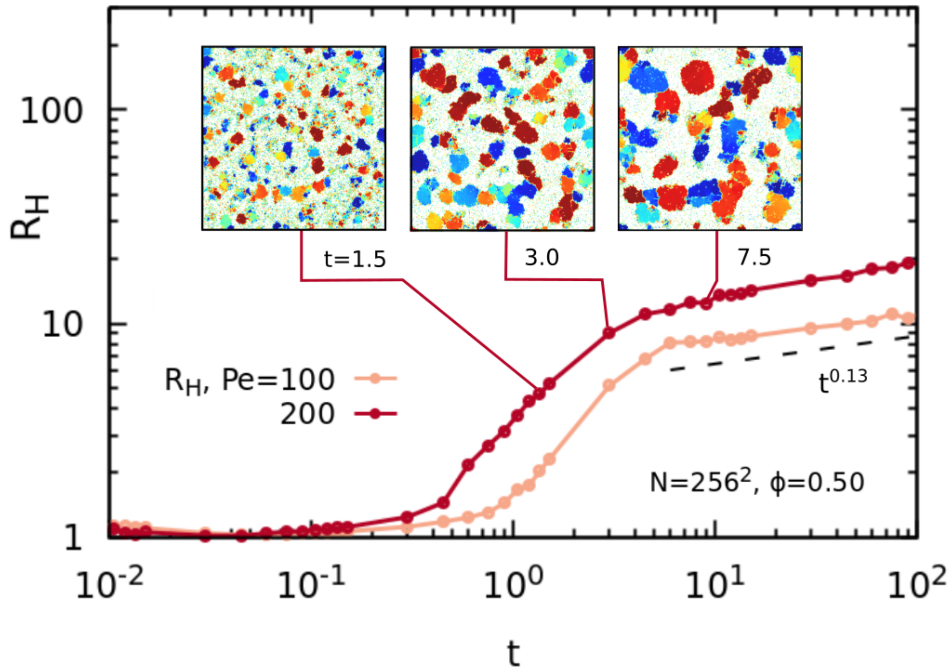

Full hexatically ordered small clusters

Larger clusters with several orientational order within

$R_H \sim t^{0.13}$ in the scaling regime and $R_H \to R_H^s \ll L$

Similar to pattern formation, e.g. **Vega, Harrison, Angelescu, Trawick, Huse, Chaikin & Register, PRE 71 061803 (2005)**

Macro vs. micro

Dense phase vs. hexatic growth

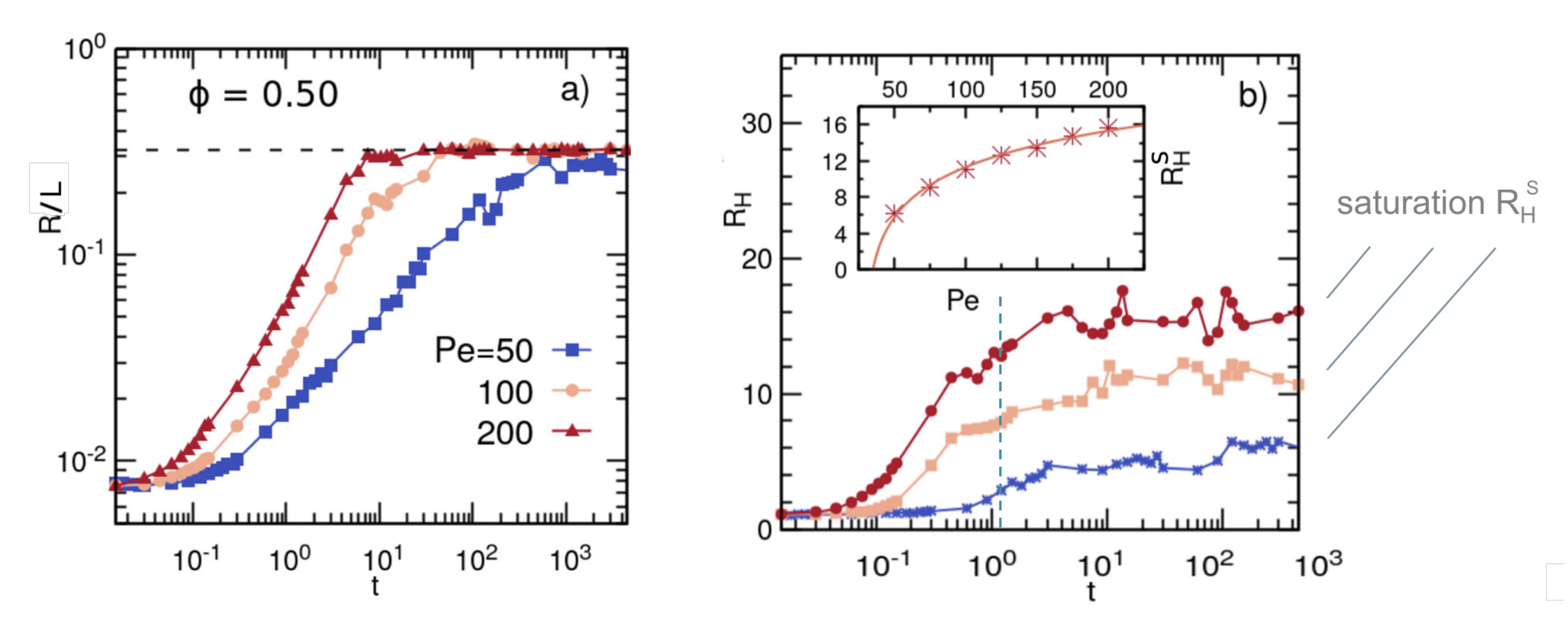

$R(t) \to aL$ $\quad$ $R_H(t) \to R_H^s$ finite

$\sim$ Exponential distribution of hexatic cluster sizes

Interfaces

Clusters of defects – mostly along hexatic-hexatic interfaces

Hexatic order map

Defects

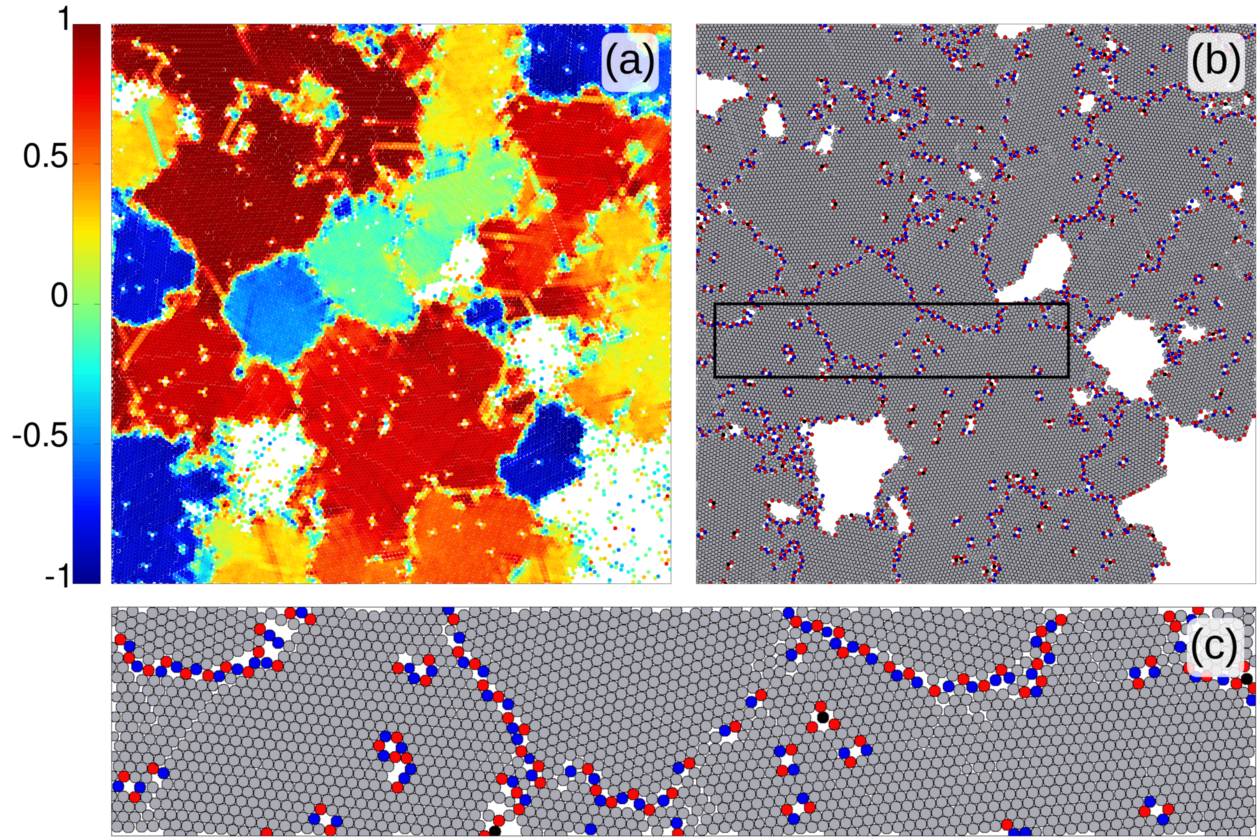

Zoom over the rectangular selection

Clusters of defects

Size distribution - Finite size cut-off

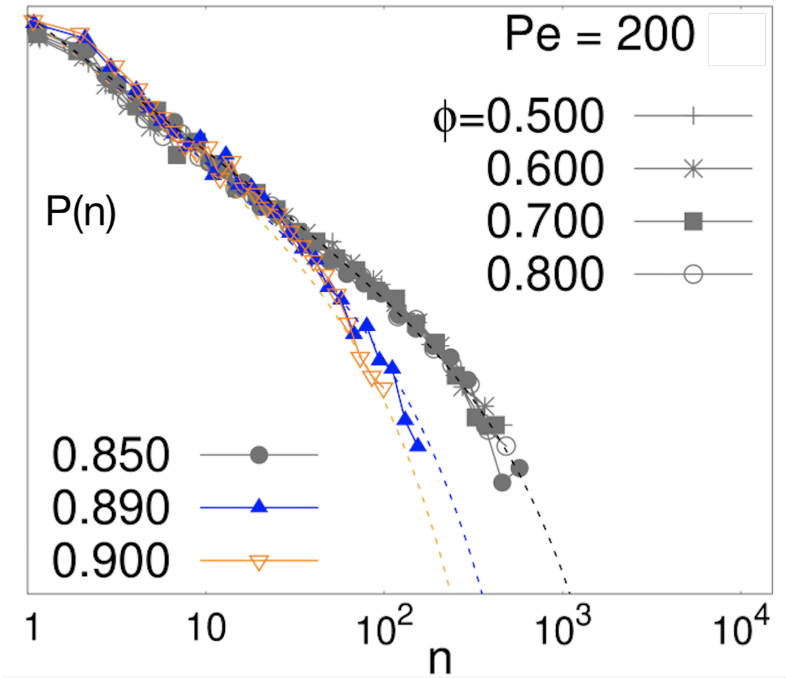

$$P(n) \simeq n^{-\tau} e^{-n/n^*}$$

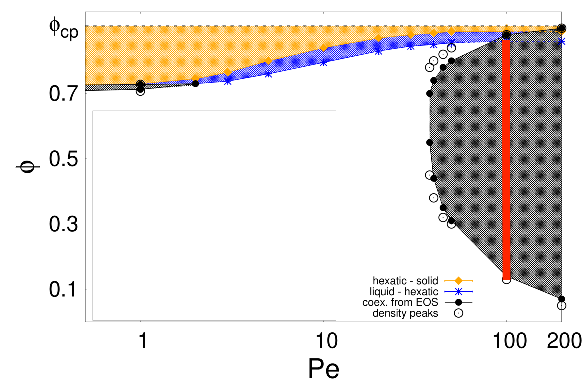

Independence of ϕ at fixed Pe within MIPS

$n^* \sim 30, 50, 200$ in the **solid**, **hexatic** and **MIPS**, respectively, and $\tau \sim 2.2$

Bubbles in cavitation

At the internal interfaces bubbles pop up

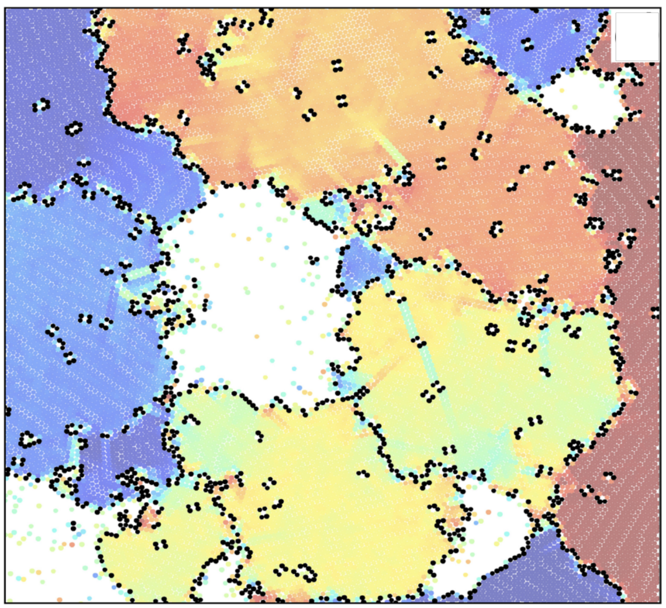

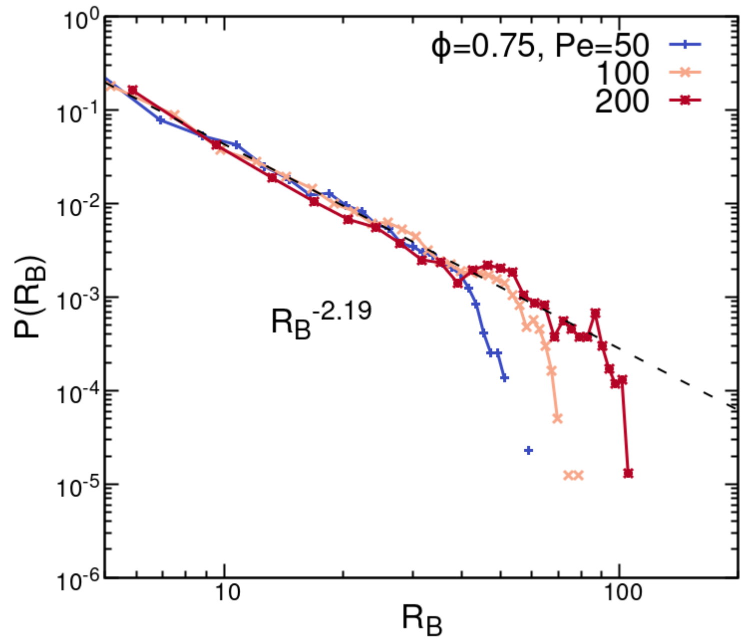

Bubbles appear and disappear at the interfaces between hexatic patches

Algebraic distribution of bubble sizes with a Pe-dependent exponential cut-off

Growth of dense components

Growth of the dense phase

Scaling of the structure factor and growth regimes

Different Pe

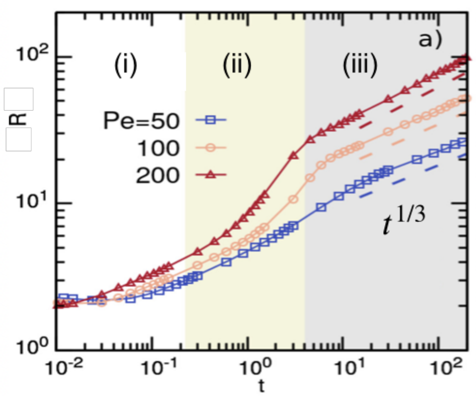

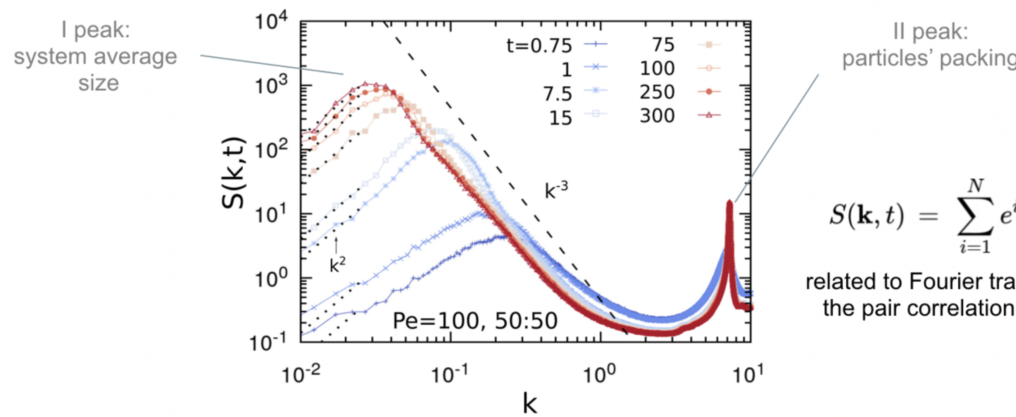

$$S(\mathbf{k},t) = \sum_{i=1}^{N} e^{i\mathbf{k}(\mathbf{r}_i - \mathbf{r}_j)}$$

related to Fourier transform of the pair correlation function

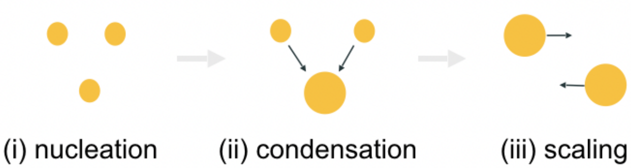

$$S(k,t) \sim R(t)^d \, f(kR(t))$$

$$R(t) \sim t^{1/3}$$

In the **scaling regime** $t^{1/3}$ like in **Lifshitz-Slyozov-Wagner**, scalar phase separation

Ostwald ripening small cluster evaporate and large ones capture gas particles

but is it just that ?

Growth of the dense phase

Focus on the clusters

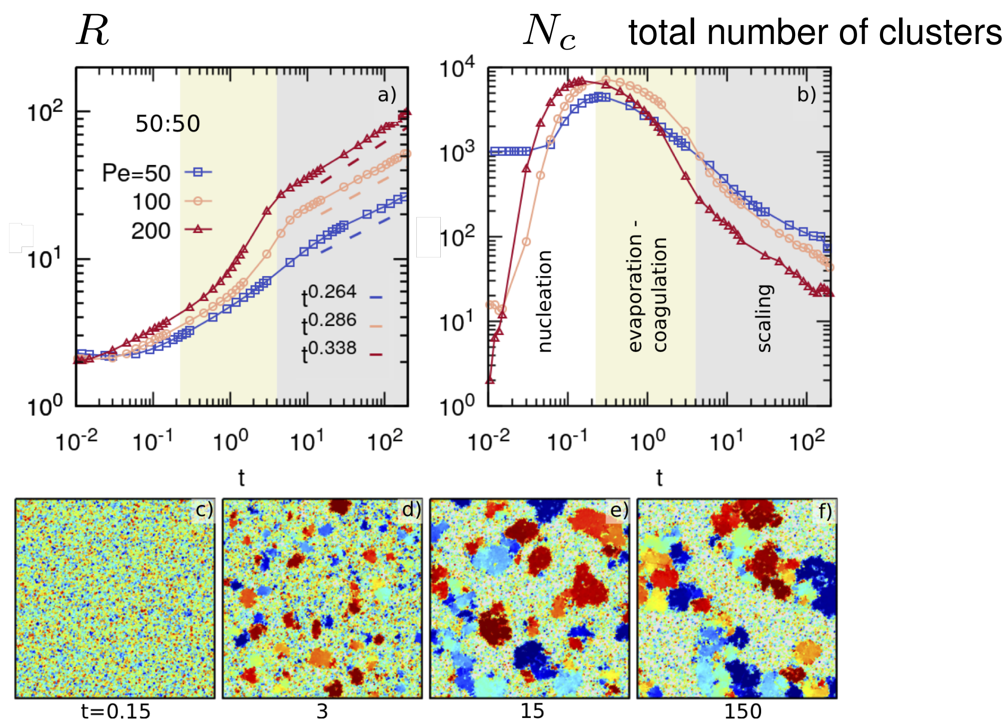

Nucleation Evap/coag Scaling

On the averaged scaling regime:

Redner, Hagan & Baskaran, PRL 110, 055701 (2013)

Stenhammar, Marenduzzo, Allen & Cates, Soft Matter 10, 1489 (2014)

Caporusso, Digregorio, Levis, LFC & Gonnella, PRL 125, 178004 (2020)

Beyond ?

Goals :

1. Is it like the one undergone by a system of **passive attractive particles** ?

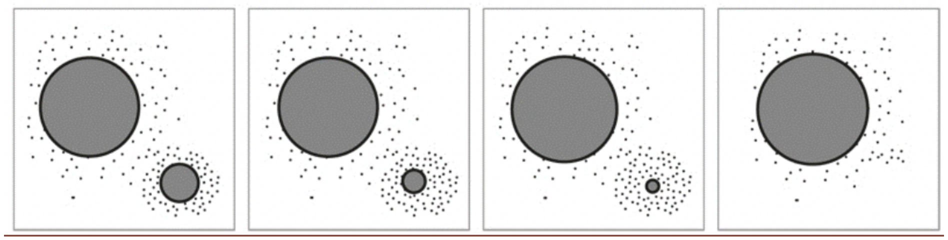

Ostwald ripening

2. Other **mechanisms** for the growth process ?

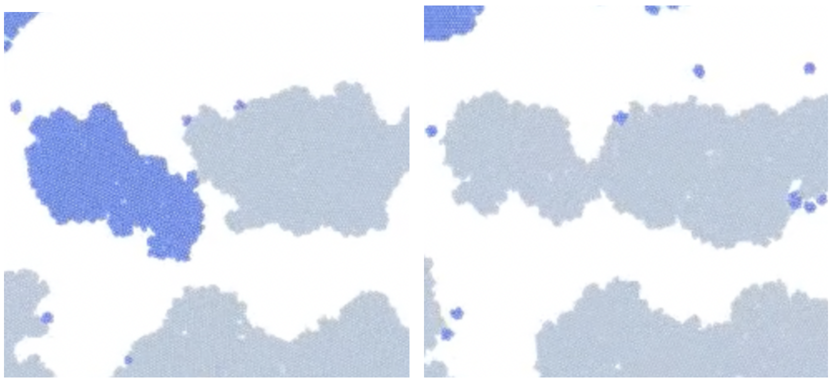

Cluster-cluster aggregation

Dense clusters

Instantaneous configurations (DBSCAN)

Passive

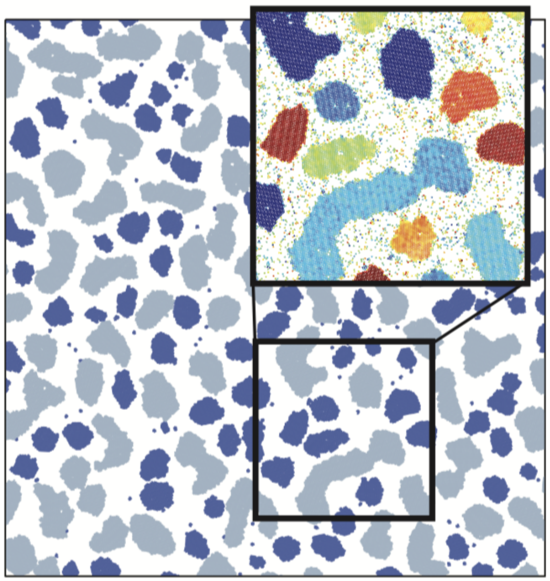

Active

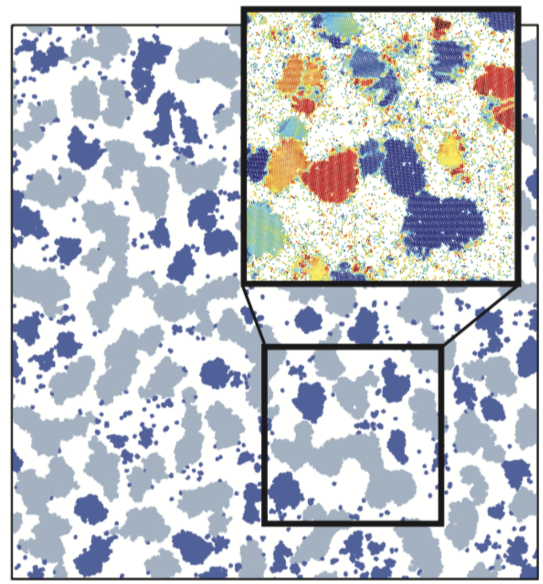

The Mie potential is not truncated in the passive case $\Rightarrow$ attractive

Parameters are such that $R(t)$ is the same

Colors in the zoomed box indicate orientational order

Caporusso, LFC, Digregorio, Gonnella, Levis & Suma, arXiv: 2211.12361

Dense clusters

Visual facts about the instantaneous configurations

Similarities

- Large variety of shapes and sizes (masses)

  Co-existence of

  small regular (**dark blue**) and large elongated (**gray**) clusters

Differences

- Rougher interfaces in active
- Homogeneous (passive) vs. heterogeneous (active) orientational order within the clusters

Cluster dynamics

Tracking of individual cluster motion - video

Active

Passive

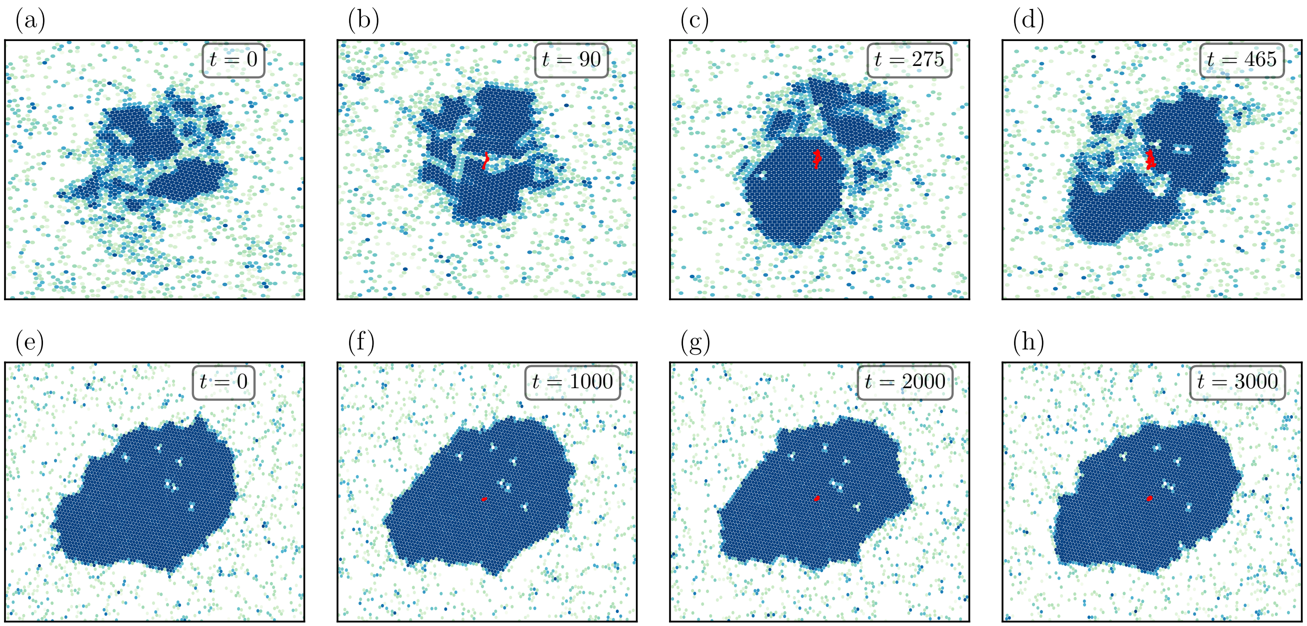

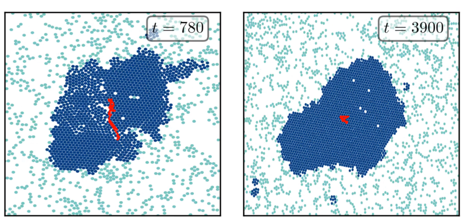

In **red** the center of mass trajectory

Active is much faster than passive

Dense clusters

Visual facts about the cluster dynamics

In both cases, **Ostwald ripening** features

- small clusters evaporate
- gas particles attach to large clusters

In the **active system**

- clusters displace much more & sometimes aggregate
- they also break & recombine

like in **diffusion limited cluster-cluster aggregation**

Dense clusters

Averaged mass $\overline{M} \equiv N_c^{-1}(t) \sum_{\alpha=1}^{N_c(t)} M_\alpha(t) \sim t^{2/3}$

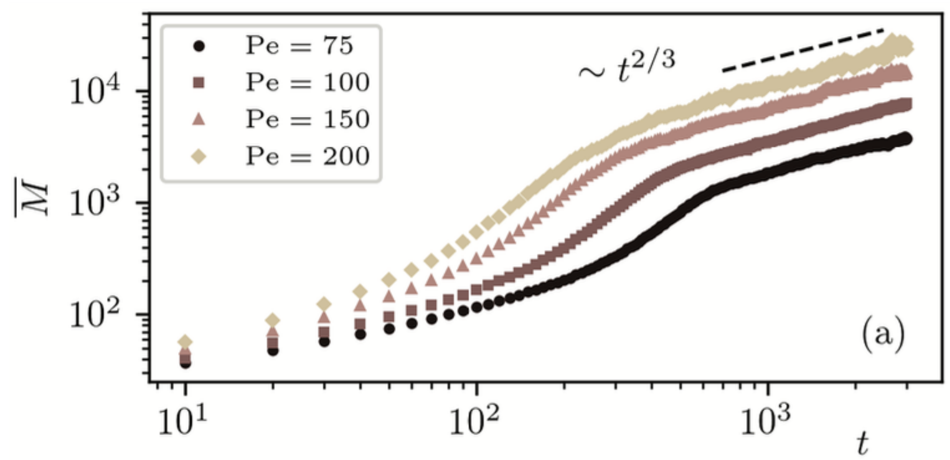

Same three regimes as in R from the structure factor

Clusters' dynamics origin ?

Active cluster evolution

Mean Square Displacement

Average over all clusters | **Mass dependence**

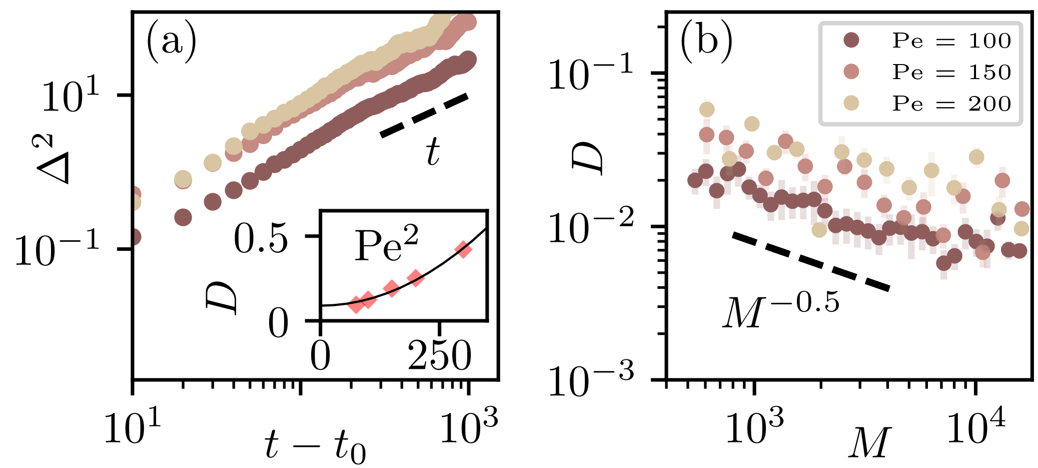

$$\Delta_k^2(t, t_0) = [\mathbf{r}^{(k)}_{\mathrm{c.o.m.}}(t) - \mathbf{r}^{(k)}_{\mathrm{c.o.m.}}(t_0)]^2 \sim 2d\, D(M_k, \mathrm{Pe})\,(t - t_0)$$

A sum of random forces yields $D \sim M^{-1}$

Passive tracer in a dilute active bath $D \sim R^{-1} \sim M^{-1/2}$ Solon & Horowitz (22)

Passive & very heavy isolated active clusters behave as $D \sim M^{-1}$

Geometry

Scatter plots: small regular – large fractal

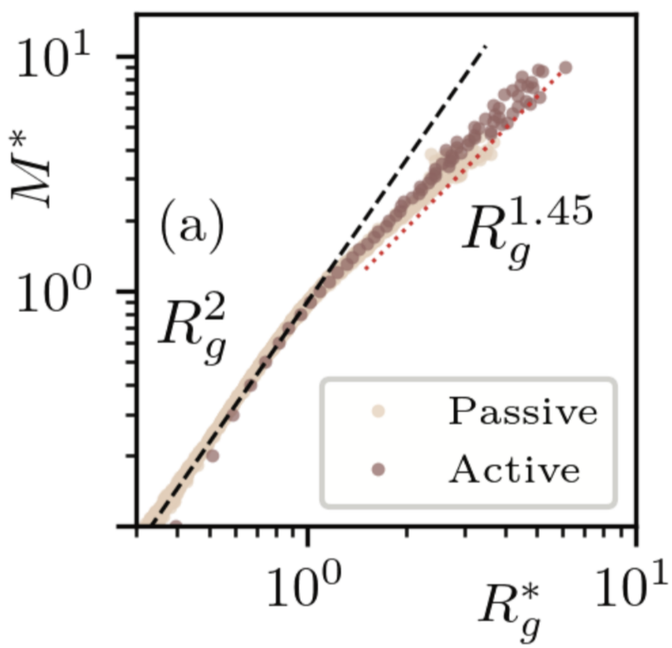

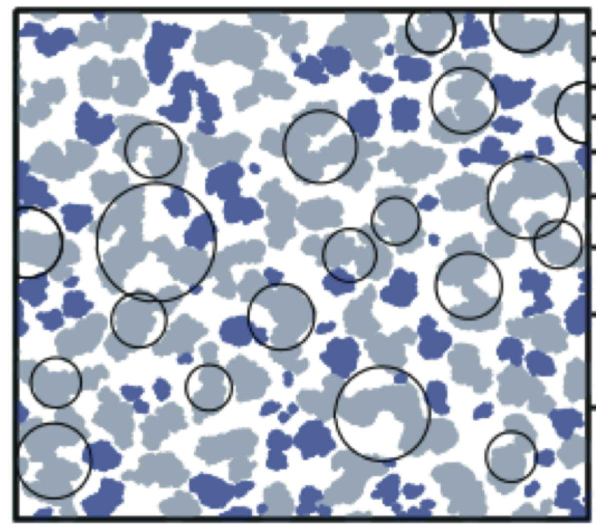

Cluster mass $M^*(t) = \frac{M_k(t)}{\overline{M}(t)}$ Gyration radius $R_g^*(t) = \frac{R_{g\,k}(t)}{\overline{R_g}(t)}$

Data sampled in the scaling regime $t = 10^3 - 10^5$ every 10^3 time steps

$\overline{M}(t) = \frac{1}{N_c(t)} \sum_{k=1}^{N_c(t)} M_k(t)$ and $N_c(t)$ the total number of clusters at time t

Cluster-cluster aggregation

Extended Smoluchowski argument

From $\overline{R}_g \sim t^{1/z}$ and using $D(M) \sim M^{-\alpha}$

Smoluchowski eq. $\Rightarrow z = d_f(1+\alpha) - (d - d_w)$

Regular clusters $M < \overline{M}$

$d_f = d = d_w = 2$

$\alpha = 0.5$

$z = 2(1 + 0.5) = 3$

Fractal clusters $M > \overline{M}$

$d_f = 1.45$, $d = 2$ and $d_w \sim 2$

$\alpha = 0.5$ in the bulk

$z = 1.45(1 + 0.5) = 2.18 < 3$

Reviews on the application of fractals to colloidal aggregation

R. Jullien, Croatia Chemica Acta 65, 215 (1992) P. Meakin, Physica Scripta 46, 295 (1992)

Regular vs fractal clusters

Radius of gyration and number

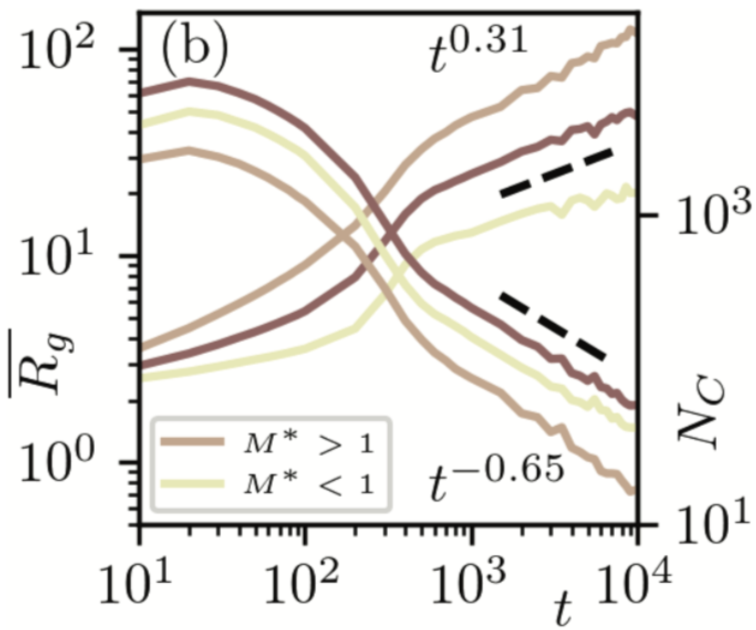

regular $z \gtrsim 3$ | fractal $z < 3$ | average $z = 1/0.31 \sim 3$

More | Less | All

Dominate

Results I

We established the full

phase diagram of ABPs

solid, **hexatic**, **liquid** & **MIPS**

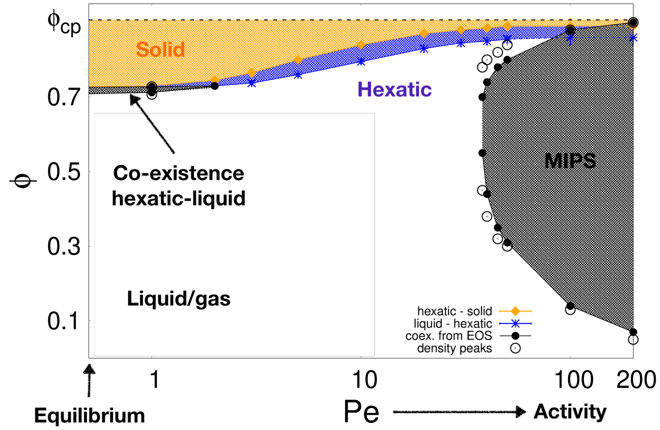

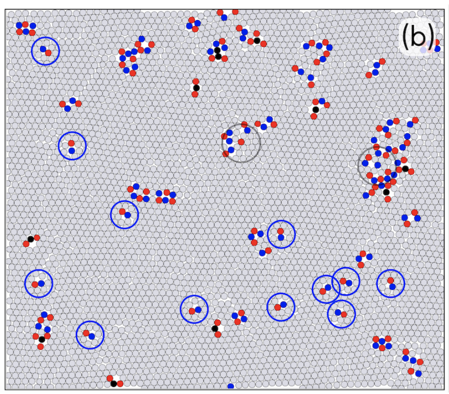

We clarified the role played by point-like

(**dislocations** & **disclinations**)

and **clustered** defects in

passive & active $2d$ models.

In **MIPS**

Micro *vs.* macro : hexatic patches & bubbles

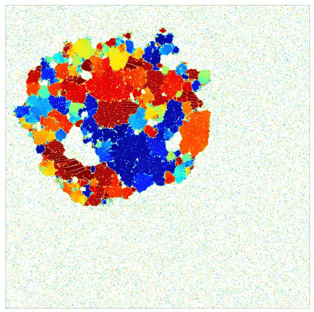

Results II

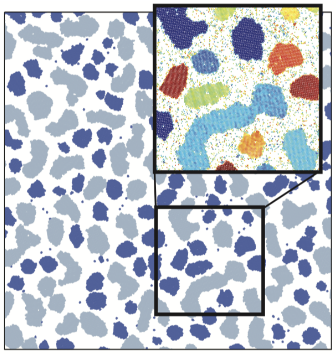

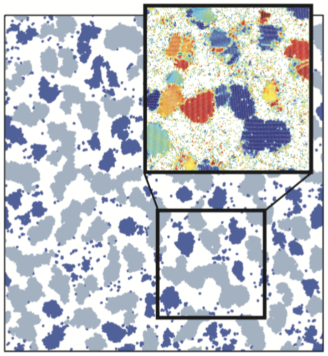

Difference between

Passive

Active

growth

Ostwald ripening & cluster-cluster aggregation in active case
cluster-cluster aggregation almost not present in passive

Co-existence of regular and fractal clusters

Heterogeneous orientational order in large active clusters

Cluster-cluster aggregation

Extended Smoluchowski argument

From $\overline{R}_g \sim t^{1/z}$ and using $D(M) \sim M^{-\alpha}$

Smoluchowski eq. $\Rightarrow z = d_f(1+\alpha) - (d - d_w)$

Regular clusters $M < \overline{M}$

$d_f = d = d_w = 2$

$\alpha = 0.5$

$z = 2(1 + 0.5) = 3$

Fractal clusters $M > \overline{M}$

$d_f = 1.45$, $d = 2$ and $d_w \sim 2$

if, instead, $\boxed{\alpha = 1}$

$z = 1.45(1 + 1) \sim 3$

Reviews on the application of fractals to colloidal aggregation

R. Jullien, Croatia Chemica Acta 65, 215 (1992) P. Meakin, Physica Scripta 46, 295 (1992)